Microelectronic Engineering 127 (2014) 86–96

Contents lists available at ScienceDirect

Microelectronic Engineering

journal homepage: www.elsevier.com/locate/mee

A fast path-based method for 3-D resist development simulation

Q. Dai [a], R. Guo [a], S.-Y. Lee [a,*], J. Choi [b], S.-H. Lee [b], I.-K. Shin [b], C.-U. Jeon [b], B.-G. Kim [b], H.-K. Cho [b]

[a] *Department of Electrical and Computer Engineering, Auburn University, Auburn, AL 36849, United States*
[b] *Samsung Electronics, Mask Development Team, Hwasung, Kyunggi-Do, 445-701, Republic of Korea*

ARTICLE INFO

Article history:
Received 28 December 2013
Received in revised form 15 March 2014
Accepted 30 April 2014
Available online 10 May 2014

Keywords:
Development paths
Lateral development
Resist development
Resist profile
Simulation
Vertical development

ABSTRACT

A three-dimensional (3-D) remaining resist profile often needs to be estimated and examined especially for nanoscale feature. However, conventional methods, such as the cell removal method and fast marching method, require intensive computation, and therefore are too time-consuming to be employed for large patterns such as a mask or an iterative procedure such as proximity effect correction (PEC). In this paper, a new method for 3-D resist development simulation has been developed for fast and accurate simulation of simple patterns such as lines and rectangles. It employs the concept of "development paths" to model the development process. In order to reduce the simulation time, each path is examined individually without a time-consuming iterative procedure which is adopted by conventional methods. An adaptive scheme has also been incorporated into the proposed simulation method, which further reduces the simulation time without sacrificing simulation accuracy substantially. The simulation results show that the proposed method achieves resist profiles well matched with those by conventional methods, even for more general patterns, but reducing simulation time by orders of magnitude, and the speed-up is larger for a larger pattern. Also, the accuracy of the proposed method has been verified experimentally.

© 2014 Elsevier B.V. All rights reserved.

1. Introduction

In a lithographic process involving resist such as electron-beam (e-beam) and optical lithographies, it is often necessary to examine the remaining resist profile after resist development. It is highly likely that the resist profile varies along the resist depth dimension. For nanoscale features, the variation is significant compared to the feature size and therefore cannot be ignored [1]. Hence, a 3-D (rather than 2-D) resist profile needs to be examined in order to take the variation into account. Also, in the case of grayscale lithography [2–4], the resist profile to be examined has to be of 3-D. In obtaining the remaining resist profile of a feature or pattern, a simulation approach is widely used, which follows the resist development process given an exposure distribution in the resist layer.

The importance of the development simulation method has been well recognized and several 2-D/3-D methods were developed. A simulator for ZEP520A in cold development was developed by Okada et al. [5]. In their model, resist dissolution is assumed only in the vertical direction, and thus it may not be accurate to simulate thicker resists or complex features due to the isotropic property of the resist development process. Stepanova et al. [6] introduced a kinetic model for resist development based on appropriate initial and boundary conditions. A numeric solution of the general mean-field equations that predict dissolution of exposed PMMA is derived as a function of time. However, the accuracy of this method heavily relies on the unknown parameters to be assumed. Two dissolution algorithms were discussed by Patsis et al. [7]. The dynamic dissolution algorithm is able to simulate the developer diffusion process explicitly, but requiring a great deal of computation. Schnattinger et al. [8] developed a stable method for discrete molecular-level mesoscopic resist simulation using an event-based dissolution algorithm. However, it is time-consuming due to its iterative procedure. Cell removal methods are widely used [9–11] because those methods have been proved to be more stable and robust, and easier to implement. The fast marching method, which efficiently implements the level set method proposed by Sethian et al. [12], is also widely used for its high accuracy in the front advancing problems [13]. The iterative simulation procedures employed in these two methods make their computational requirement high, especially for development simulation of 3-D resist profile.

There are many applications where it is not practical to employ a time-consuming simulation method for obtaining resist profiles. One example is estimation of the 3-D resist profile of a large

* Corresponding author. Fax: +1 (334) 844 1809.
E-mail address: leesooy@eng.auburn.edu (S.-Y. Lee).

http://dx.doi.org/10.1016/j.mee.2014.04.046
0167-9317/© 2014 Elsevier B.V. All rights reserved.

pattern which would be a necessary step in optimizing the lithographic process before actual fabrication of the large pattern, such as photomask or imprint lithography mold, using e-beam lithography. Another is the proximity correction, e-beam or optical, where the resist development simulation needs to be carried out in each iteration of an iterative correction procedure [3,4,14–19]. Note that for true 3-D correction of nanoscale features, the critical dimension such as line width needs to be measured at each layer of resist. This layer-by-layer analysis of resist profile would not be needed in a conventional 2-D correction. Therefore, there exists a practical need for a fast and accurate method to simulate resist development process for obtaining 3-D resist profiles. Also, it is often sufficient to examine the cross-section of resist profile for simple features in order to measure the critical dimension of feature such as line width without paying much attention to fine detail.

In this study, in order to meet the above-mentioned need, a fast path-based method for 3-D resist development simulation of simple patterns such as lines and rectangles, which avoids the time-consuming computation without sacrificing the simulation accuracy, has been developed. The key idea of the proposed method is that the development process can be modeled by "development paths," i.e., paths starting from the top surface of resist toward the boundaries of the final resist profile. Given a developing time, all possible paths are individually examined without any iterative procedure and a set of the paths reaching the farthest points on individual layers of resist determines the resist profile. Although the actual development paths may not be the same as those in the path-based method, consideration of all possible paths starting from (all points on) the resist surface (and the boundary of resist profile is determined by the set of square paths reaching the farthest points) tends to compensate for the potential discrepancy between the simulated paths and actual paths. Through an extensive simulation, the proposed path-based method is compared with the cell removal and fast marching methods in terms of simulation time and accuracy. It turns out that the resist profiles obtained by the proposed path-based method are well matched with those by the cell removal and fast marching methods, even in more general shapes of patterns (than lines and rectangles), and the simulation time can be reduced by orders of magnitude, a larger reduction for a larger pattern. Also, the cross-section of resist profile of a line obtained through an experiment is shown to be very close to the one by the path-based method.

The rest of the paper is organized as follows. The related model is briefly described in Section 2. The conventional methods (cell removal and fast marching methods) are briefly discussed in Section 3. The proposed path-based method is described in Section 4. The adaptive procedure for optimizing the tradeoff between simulation accuracy and time is described in Section 5. Simulation results are discussed in Section 6, followed by a summary in Section 7.

2. Model

2.1. Exposure model

In a typical substrate system employed in this study, a resist layer with initial thickness of H is on top of the substrate, as illustrated in Fig. 1 where the X–Y plane corresponds to the top surface of resist and the resist depth is along the Z-dimension. The 3-D PSF is denoted by $\mathrm{psf}(x,y,z)$ which describes the distribution of energy deposited (exposure) in the resist when a single point is exposed. Let $d(x,y,0)$ represent the e-beam dose given to the point $(x,y,0)$ on the surface of the resist for writing a circuit feature or pattern (refer to Fig. 1). For example, in the case of a uniform dose distribution,

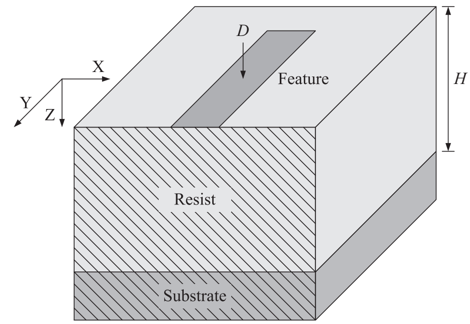

Fig. 1. Illustration of the substrate system where H is the initial thickness of resist.

$$d(x,y,0)=\begin{cases} D & \text{if } (x,y,0) \text{ is within a feature} \\ 0 & \text{otherwise} \end{cases} \tag{1}$$

where D is a constant dose.

Let us denote the exposure at the point (x,y,z) in the resist by $e(x,y,z)$. Then, the 3-D spatial distribution of exposure can be expressed by the following convolution:

$$e(x,y,z)=\iint d(x-x',y-y',0)\mathrm{psf}(x',y',z)dx'dy'. \tag{2}$$

From Eq. 2, it can be seen that the exposure distribution at a certain depth z_0 can be computed by the 2-D convolution between $d(x,y,0)$ and $\mathrm{psf}(x,y,z_0)$ in the corresponding plane $z=z_0$, i.e., $e(x,y,z)$ may be estimated layer by layer. Note that the PSF, $\mathrm{psf}(x,y,z)$, reflects all the phenomena affecting energy deposition including the e-beam blur.

2.2. Exposure-to-rate conversion formula

During the writing process on a PMMA resist, the electrons come across the resist and deposit energy (exposure) which ionizes the phenol groups in the polymer. Each initially blocked (protected) phenol group in the polymer has a chance to be ionized. If the number of ionized phenol groups exceeds the critical fraction, the polymer becomes soluble [20]. The probability of a given phenol group being ionized is directly related to the exposure deposited in that group, and thus the developing rate at each point in the resist can be subsequently derived from the exposure at that point. The developing rate is also related to many other factors such as molecular weight and pH of the developer. Most resists are nonlinear in nature when exposed by the e-beam, i.e., the developing rate is not linearly proportional to the exposure. Therefore, the developing rate $r(x,y,z)$ at each point in the resist is calculated from its corresponding exposure $e(x,y,z)$ through a nonlinear exposure-to-rate conversion formula $F[\cdot]$ which may be derived experimentally.

The conversion formula may be derived experimentally as follows. A single line is exposed with a spatially-uniform dose, and after resist development, the depth in the cross-section of remaining resist profile is measured at the center of line. This process is repeated with different dose levels. Note that the resist is developed only vertically at the center of line when the dose is spatially uniform. The resist profile can also be obtained through simulation by computing the exposure distribution in the resist and converting exposure into developing rate. The relationship between exposure and developing rate (i.e., conversion formula), which minimizes the difference between the measured and simulated depths, is obtained. The following conversion formula $F[\cdot]$ was derived (also refer to Fig. 2) using the experimental results where substrate system is composed of 300 nm PMMA on Si:

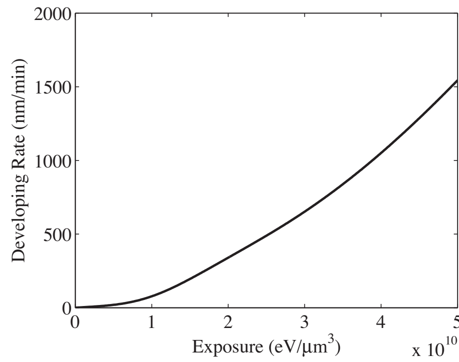

Fig. 2. The experiment-based nonlinear exposure-to-rate conversion formula $F[\cdot]$.

$$r(x,y,z) = F[e(x,y,z)] = 4000 \cdot e^{-\left(\frac{e(x,y,z)-1.0e11}{5.8e10}\right)^2} + 50 \cdot e^{-\left(\frac{e(x,y,z)-7.0e9}{1.0e10}\right)^2} - 235, \quad (3)$$

where $r(x,y,z)$ is in nm/min and $e(x,y,z)$ in eV/μm^2. The validity of this conversion formula was verified in our previous work [21].

3. Existing methods

In this section, two of the existing methods widely used are described, to which the proposed path-based method is compared.

3.1. Cell removal method

A standard cell removal method is implemented for comparison in this study. In the 3-D version of the cell removal method, the resist layer is partitioned into cubic cells as shown in Fig. 3, and the exposure in each cell is computed and converted into the developing rate. The developing process is started from the top surface. In each iteration of the simulation, the surface (sides) of a cell that is in contact with the developer is determined and each side is adjusted based on the developing rate. If a cell is fully developed, the states of its neighbors are updated, i.e., mores sides are considered to be exposed to the developer or the undeveloped cells start to be developed. Given a specified developing time, the remaining resist profile can by derived from the boundary between the developed and undeveloped cells.

3.2. Fast marching method

A fast marching level set method is initially proposed to handle monotonically advancing fronts problems by solving the Eikonal equation. It is based on level set methods which are numerical techniques for computing the position of propagating fronts. It relies on an initial value partial differential equation for propagating a level set function and uses techniques borrowed from hyperbolic conservation laws [12].

In the beginning of the fast marching method, the developing times of the source points (on the resist surface) are set to be 0, and they are marked as developed points whereas all other points are set as undeveloped points. In each iteration, the neighbors of the developed points are added into the front list, and their developing times are derived by solving the Eikonal equation. Only the point with the smallest developing time is marked as developed and its undeveloped neighbors are added into the front list for the next iteration. After deriving the developing times of all points, the remaining resist profile can be derived from a specified developing time.

4. Proposed path-based method

In this study, a novel method for 3-D resist development simulation has been proposed in order to reduce the simulation time of an iterative method such as the cell removal method. The proposed method employs the concept of "development paths," which start from the top surface of resist toward the boundaries of the final resist profile, to model the development process.

The resist development process is isotropic as the resist is developed in all possible directions. However, in the proposed method, the development process is modeled by two orthogonal processes, i.e., vertical development and lateral development, in order to simplify the simulation procedure. Accordingly, each development path (just path hereafter) consists of two orthogonal path segments, i.e., vertical (to depict vertical development) and lateral (to depict lateral development) path segments (refer to Fig. 4). More specifically, each path has one vertical path segment

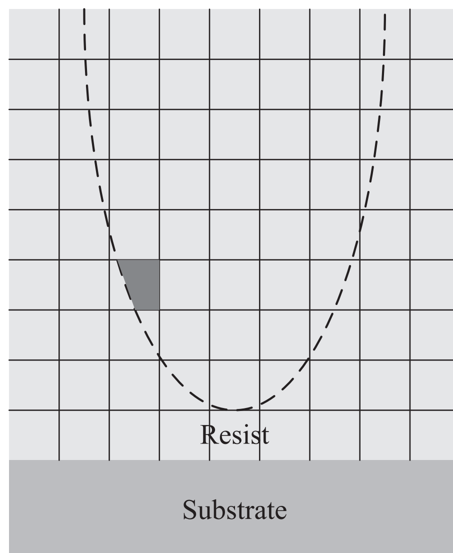

Fig. 3. Illustration of the cell removal method where the dashed curve represents a cross-section of resist profile.

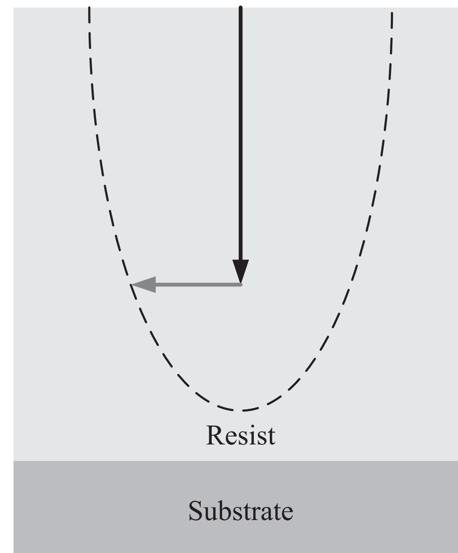

Fig. 4. Illustration of the path-based method where the dashed curve represents a cross-section of resist profile.

(along the Z-dimension) and may have one or more lateral path segments (along the X-dimension or Y-dimension). Note that the vertical path segment only would not lead to an accurate resist profile since the lateral development is not taken into account (refer to Fig. 5).

Each path is "computed" (followed) individually, i.e., finding out the farthest point in the resist a path can reach given a developing time T. The computation of a path starts by considering its vertical path segment, followed by its lateral path segments. A path makes a turn when it switches from a vertical path segment to a lateral path segment or a lateral path segment to another lateral path segment. Whether and in what direction a path is to be turned at a point depends on the relative developing rates of adjacent points in the X–Y (horizontal) plane. When a point has a higher developing rate than its neighboring point, it is developed faster leading to lateral development toward the neighboring point. The larger the difference of developing rate is, the larger the lateral development is. Therefore, the turn of a path is always from a point with a higher developing rate to its neighboring point(s) with a lower developing rate in the X–Y plane.

Let the distances between adjacent points in the X-dimension, Y-dimension, and Z-dimension be denoted by $\Delta x, \Delta y$, and Δz, respectively. A turn is allowed only from one point (x, y, z) with a higher developing rate to its adjacent points with lower developing rates, i.e., $r(x, y, z) > r(x + \Delta x, y, z)$ or $r(x, y, z) > r(x - \Delta x, y, z)$ or $r(x, y, z) > r(x, y + \Delta y, z)$ or $r(x, y, z) > r(x, y - \Delta y, z)$. For example, a path turns into the positive X-direction only at the point (x, y, z) if $r(x, y, z) > r(x + \Delta x, y, z)$ but $r(x, y, z) \leqslant r(x - \Delta x, y, z)$, as illustrated in Fig. 6(a). But, if $r(x, y, z) > r(x + \Delta x, y, z)$ and $r(x, y, z) > r(x - \Delta x, y, z)$, it turns into both the positive and negative X-directions, as illustrated in Fig. 6(b).

In general, the more turns allowed, the more accurate the simulation result becomes, but the longer the simulation time is. It is found that in many cases, one turn is sufficient to achieve high accuracy of simulation, e.g., when one is interested only in cross-sections of resist profile for a line feature. Even for more general shapes of feature, two turns are sufficient to obtain accurate 3-D resist profiles at the expense of a longer simulation time compared to the case where only one turn is allowed (refer to Fig. 7).

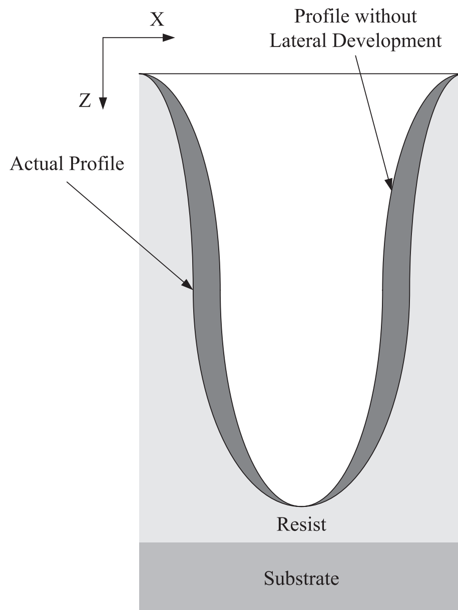

Fig. 5. The difference between the actual resist profile and the resist profile without considering the lateral development.

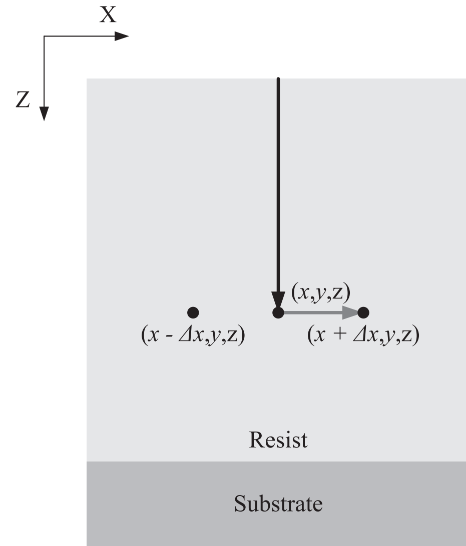

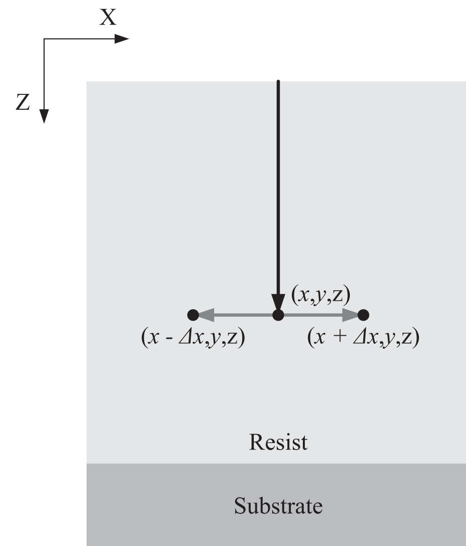

Fig. 6. A path turns to (a) only the positive direction of the X-axis at the point (x, y, z) if $r(x, y, z) > r(x + \Delta x, y, z)$ but $r(x, y, z) \leqslant r(x - \Delta x, y, z)$ and (b) both the positive and negative directions of the X-axis at the point (x, y, z) if $r(x, y, z) > r(x + \Delta x, y, z)$ and $r(x, y, z) > r(x - \Delta x, y, z)$.

The computation of each path terminates when the sum of the times spent on its path segments is equal to the given developing time T, which is given by (refer to Fig. 8):

$$\sum_{z=0}^{z'} \frac{\Delta z}{r(x_0, y_0, z)} = T, \tag{4}$$

for no-turn (vertical-only) paths,

$$\sum_{z=0}^{z_0} \frac{\Delta z}{r(x_0, y_0, z)} + \sum_{x=x_0}^{x'} \frac{\Delta x}{r(x, y_0, z_0)} = T, \tag{5}$$

for one-turn paths, and

$$\sum_{z=0}^{z_0} \frac{\Delta z}{r(x_0, y_0, z)} + \sum_{x=x_0}^{x_1} \frac{\Delta x}{r(x, y_0, z_0)} + \sum_{y=y_0}^{y'} \frac{\Delta y}{r(x_1, y, z_0)} = T, \tag{6}$$

for two-turn paths, respectively.

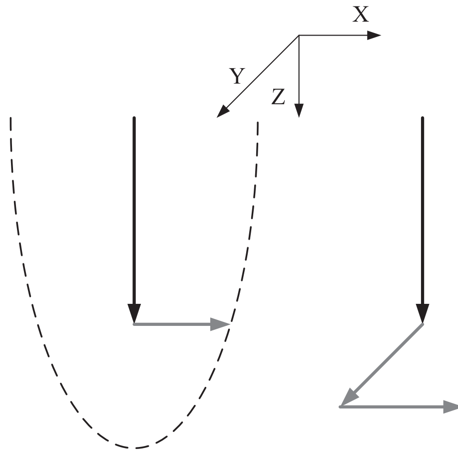

Fig. 7. The development paths with one and two turns where the black and gray lines are the vertical and lateral path segments, respectively, and the dashed curve represents a cross-section of resist profile. The Z-axis corresponds to the resist depth dimension.

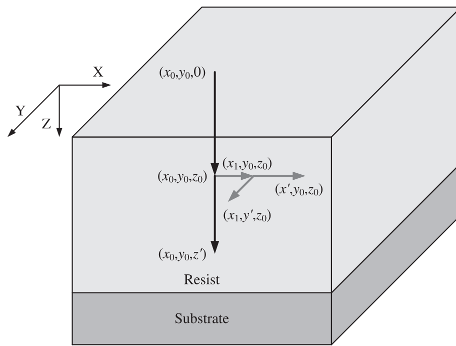

Fig. 8. The computation of each path terminates when the sum of the time spent on its path segments is equal to the given developing time T.

In order to derive the final resist profile, a mark is used to represent the status of each point during the resist development simulation. Initially, all the points in the resist are marked as "undeveloped." After each path is computed, the points which it passes through are marked as "developed." The final resist profile is determined by tracing the boundaries between the developed and undeveloped points after all possible paths are computed (refer to Fig. 9).

The complete procedure of the path-based method is depicted below (also refer to the flowchart in Fig. 10).

Step 1 : Compute the exposure distribution $e(x,y,z)$, and convert it into the developing rate distribution $r(x,y,z)$ through the conversion formula $F[\cdot]$ in Eq. 3.

Step 2 : Compute a vertical path segment along the Z-dimension starting from a point $(x_0,y_0,0)$ on the top surface of resist using the developing rate distribution $r(x,y,z)$ and the given developing time T, such that $\sum_{z=0}^{z'} \frac{\Delta z}{r(x_0,y_0,z)} = T$.

Step 3 : Compute a lateral path segment along the X-dimension starting from a point (x_0,y_0,z_0) $(0 < z_0 < z')$ on the vertical path segment obtained in Step 2 (if $r(x_0,y_0,z_0) > r(x_0+\Delta x,y_0,z_0)$ or $r(x_0,y_0,z_0) > r(x_0-\Delta x,y_0,z_0)$) such that $\sum_{z=0}^{z_0} \frac{\Delta z}{r(x_0,y_0,z)} + \sum_{x=x_0}^{x'} \frac{\Delta x}{r(x,y_0,z_0)} = T$.

Step 4 : Compute a lateral path segment along the Y-dimension starting from each point (x_1,y_0,z_0) $(x_0 < x_1 < x')$ on the lateral path segment obtained in Step 3 (if $r(x_1,y_0,z_0) > r(x_1,y_0+\Delta y,z_0)$ or $r(x_1,y_0,z_0) > r(x_1,y_0-\Delta y,z_0)$) such that $\sum_{z=0}^{z_0} \frac{\Delta z}{r(x_0,y_0,z)} + \sum_{x=x_0}^{x_1} \frac{\Delta x}{r(x,y_0,z_0)} + \sum_{y=y_0}^{y'} \frac{\Delta y}{r(x_1,y,z_0)} = T$.

Step 5 : A path is represented in the form of a vector in the 3-D space as $\boldsymbol{p} = (p_x,p_y,p_z)$, where $p_x = |x_1 - x_0|, p_y = |y'^8 - y_0|$, and $p_z = z_0$ are the lengths of the three path segments in the X-dimension, Y-dimension and Z-dimension, respectively.

Step 6 : Mark the points which the path passes through as "developed" using $\boldsymbol{p} = (p_x,p_y,p_z)$.

Step 7 : If all the possible paths are computed, proceed to Step 8. Otherwise, go back to Step 2.

Step 8 : Determine the final resist profile by tracing the boundaries between the developed and undeveloped points.

In the conventional methods, the statuses of the points in the resist exposed to the developer are incrementally updated through many iterations of small time intervals. That is the main reason why it is time-consuming. It should be clear that the proposed path-based method does not require such iterations and incremental updating. This reduces simulation time greatly, still achieving high accuracy of simulation.

5. Adaptive procedure

In order to minimize the simulation time while achieving high accuracy of simulation, an adaptive approach is incorporated into the simulation procedure. Before the final stage of simulation (resist development), the resist profile would be usually smooth without sharp shapes such as corners and junctions. Therefore, a developing period (time) is partitioned into two phases as illustrated in Fig. 11. In the first phase $(0 < t \leqslant T_0)$, only one turn is allowed for fast simulation of the early part of resist development, and in the second phase $(T_0 < t \leqslant T)$, two turns are allowed to enhance the accuracy of corners, edges, and junctions. The complexity of feature shape is to be considered in determining T_0. In general, the simpler the feature shape is, the larger T_0 should be, i.e., closer to the simulation with one turn leading to faster simulation. This adaptive approach reduces the simulation time greatly without sacrificing simulation accuracy substantially.

6. Results and discussion

The proposed path-based method for 3-D resist development simulation has been implemented and its performance has been compared with the cell removal and fast marching methods in terms of simulation accuracy and time.

In order to demonstrate that the proposed path-based method can compensate the actual isotropic development process by using a vertical path segment followed by lateral path segments, a radially-symmetric (in the cross-section perpendicular to the length dimension of the feature) exposure distribution is generated (assumed) for a long line as shown in Fig. 12(a). Note that such an exposure distribution would make the difference (if any) between the simulated (by the path-based method) and actual isotropic paths. Nevertheless, as shown in Fig. 12(b), the remaining resist profile obtained by the path-based method is very close to those by the cell removal and fast marching methods.

Eight different test patterns (Patterns I-VIII) including Pattern I (shown in Fig. 13)(a) and Pattern II (shown in Fig. 13(b)) are considered in the comparison. The largest size of pattern for simulation is 1 μm by 1 μm.

The PSFs used in the simulation are generated by a Monte Carlo simulation method, SEEL [22]. The substrate system assumed in

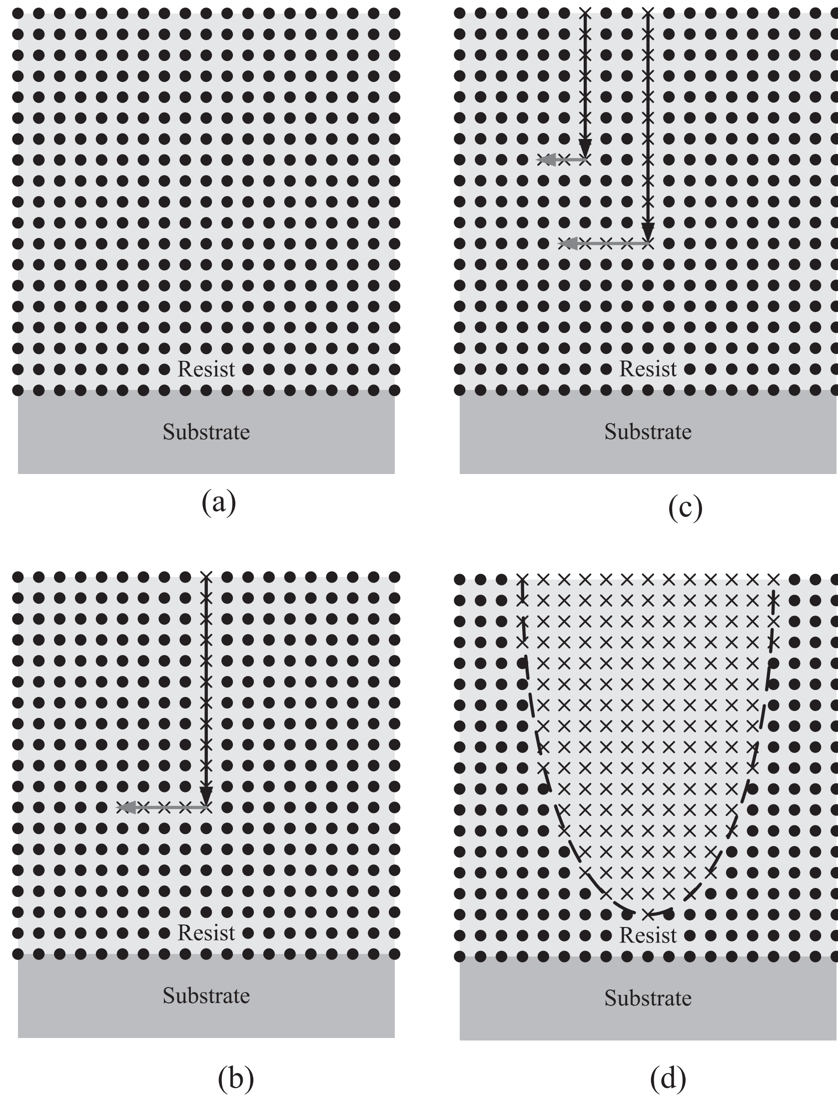

Fig. 9. (a) All the points in the resist are marked as "undeveloped" before the resist development simulation. (b) After one path is computed, the points which it passes through are marked as "developed". (c) After another path is computed, more points are marked as "developed". (d) The final resist profile is determined by tracing the boundaries between those developed points and those which are not.

this comparison is composed of 300 nm PMMA on Si. The beam energy is set to 50 keV with the beam diameter of 5 nm. It is assumed that the resist is developed in the developing system of methylisobutyl ketone (MIBK): IPA (isopropyl alcohol) = 1:3 for 60 s and IPA for 40 s at 21 °C.

The resist profiles obtained by the proposed path-based method (with the adaptive procedure) are compared with those by the cell removal and fast marching methods with the constraint that the resolution of the resist profile is the same for all three methods, which is 1 nm at the sub-pixel level. The (top-view) contours of resist profiles at the top, middle, and bottom layers, obtained for Pattern I and Pattern II, are provided in Fig. 14 and Fig. 15. Also, the cross-sections of resist profiles for Pattern IV are shown in Fig. 16. In these figures, it can be seen that the resist profiles by the proposed method are well matched with those by the cell removal and fast marching methods.

The proposed method is also compared with the cell removal and fast marching methods quantitatively in terms of the profile difference.

$$\text{Profile difference} = \frac{\sum_{x,y}|P(x,y) - C(x,y)|}{\sum_{x,y}C(x,y)} \times 100\%, \tag{7}$$

where $P(x,y)$ and $C(x,y)$ are the 2-D profile arrays (a layer for a fixed z, i.e., the top, middle, or bottom layer) of the proposed method and the cell removal method or fast marching method, respectively. The value of $P(x,y)$ and $C(x,y)$ can be either 0 (for those marked as "undeveloped") or 1 (for those marked as "developed"). The profile differences between the path-based method and the cell removal and fast marching methods are provided in Table 1. The same high accuracy is observed in all of the test patterns.

In Table 2, the simulation time measured on a PC with a 2.53 GHz CPU (Intel Core i5-540M) and 2 GB memory is provided for the test patterns. It can be seen that the proposed path-based method takes much less time for simulation, compared to the cell removal and fast marching methods. As the pattern size increases, the simulation time increases much faster for the cell removal and fast marching methods than for the path-based method. Note that the simulation time of the proposed method is almost linearly proportional to the pattern size. Hence, as can be seen from Table 3, the speedup by the proposed method over the cell removal and fast marching methods is significantly larger for a larger pattern.

The accuracy of the proposed method has also been examined experimentally. A long line with the width of single pixel was exposed with a dose of 2500 μC/cm^2 on 300 nm PMMA on Si using

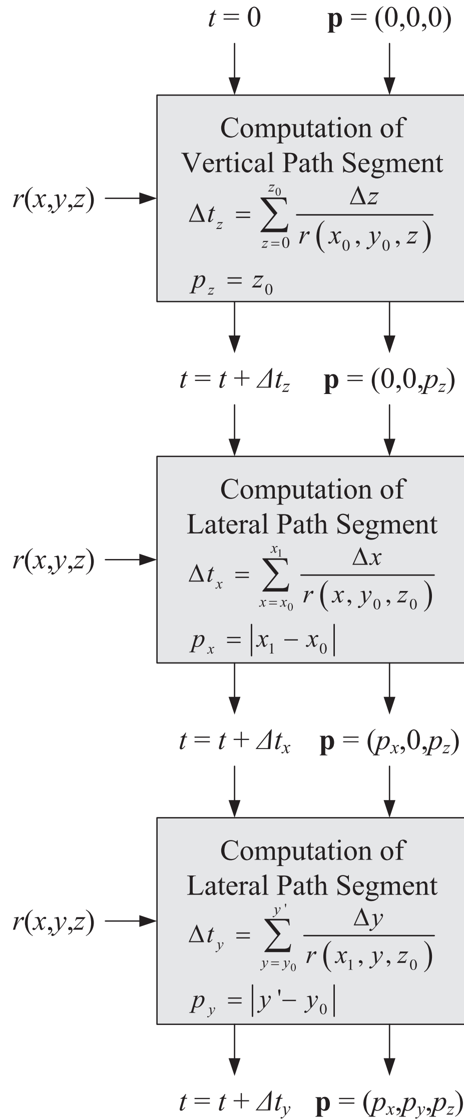

Fig. 10. Flowchart of the computation of a two-turn path, where Δt_x, Δt_y, and Δt_z ($\Delta t_x + \Delta t_y + \Delta t_z = T$) are the time spent on each path segment in the X-dimension, Y-dimension, and Z-dimension, respectively.

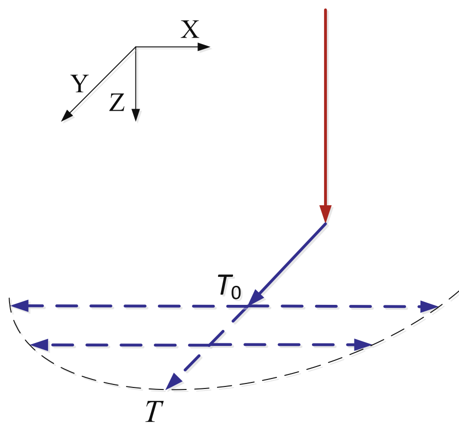

Fig. 11. Illustration of adaptive procedure where the red and blue lines are the vertical and lateral path segments, respectively. The solid blue lines and dashed blue lines are the path segments in the first phase and second phase, respectively. The dashed curve represents a cross-section of resist profile. (For interpretation of the references to colour in this figure legend, the reader is referred to the web version of this article.)

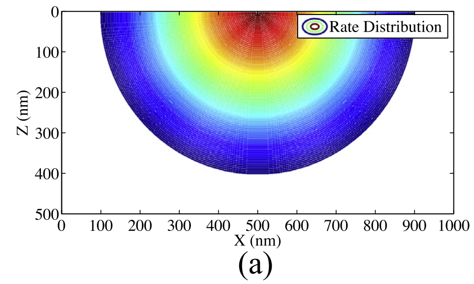

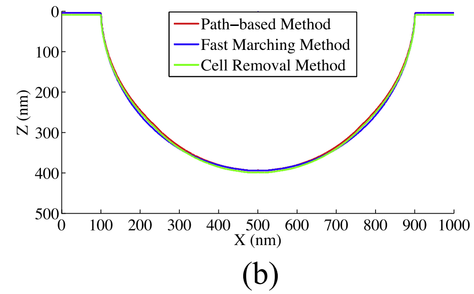

Fig. 12. (a) Radially symmetric exposure (developing rate) distribution in the cross-section (perpendicular to the length dimension of the line) of resist for a long line, and (b) the remaining resist profiles (in the cross-section) derived by path-based, fast marching, and cell removal methods.

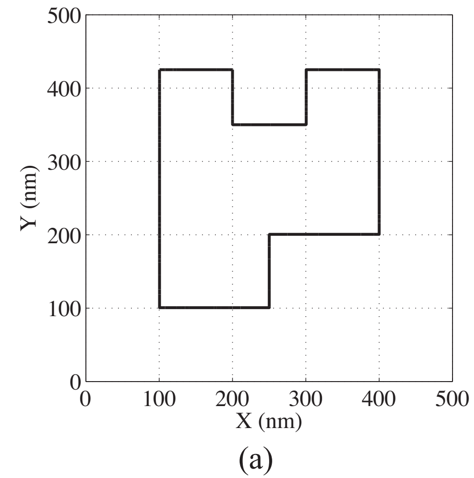

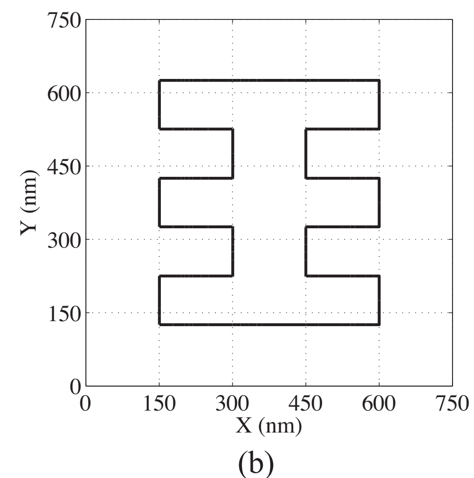

Fig. 13. The layouts of (a) Pattern I and (b) Pattern II.

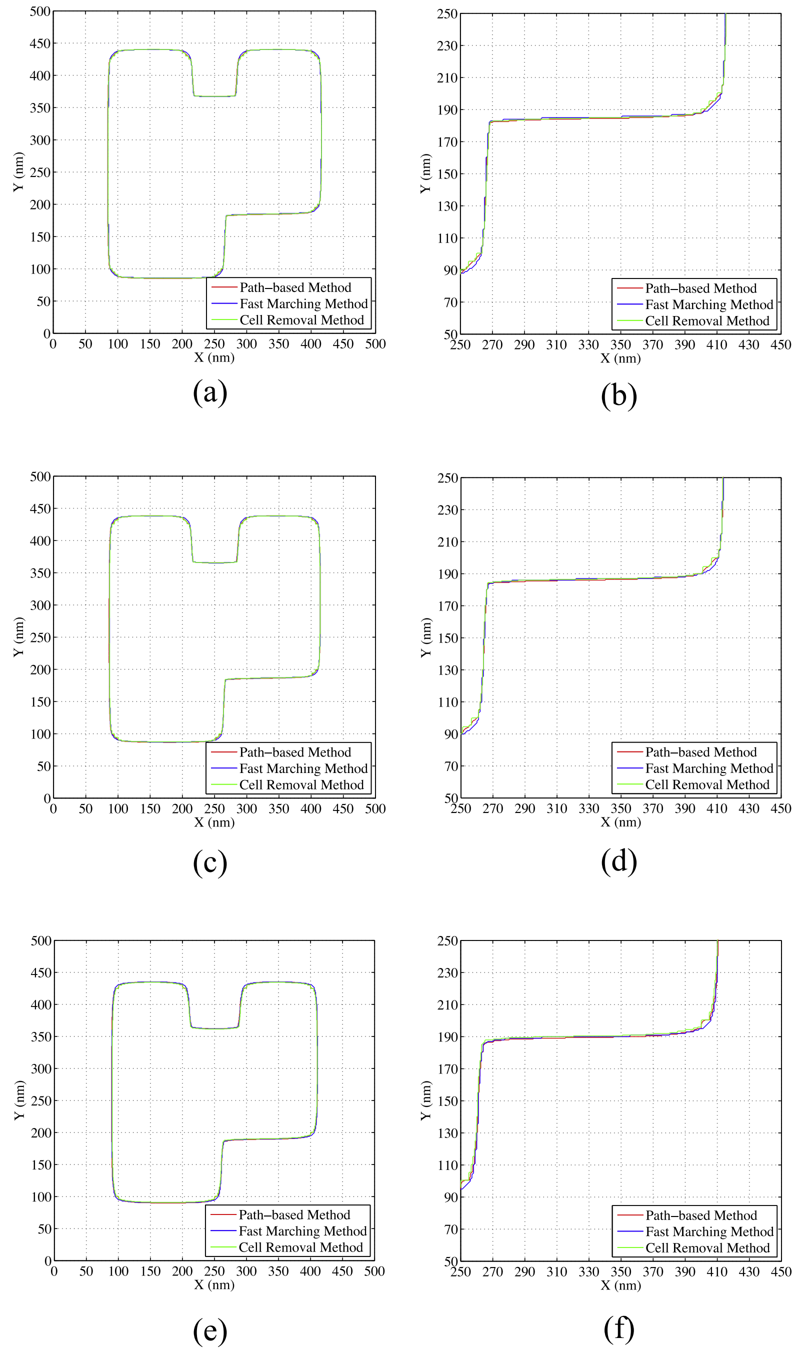

Fig. 14. The remaining resist profiles (top view) for Pattern I at the (a) top, (c) middle, and (e) bottom layers of resist by the path-based, fast marching, and cell removal methods, respectively, and the respective zoomed-in details at the (b) top, (d) middle, and (f) bottom layers.

the ELIONIX ELS-7000 e-beam lithography system. The e-beam energy was 50 keV and the sample was developed in MIBK:IPA = 1:2 for 40 s. The cross-section SEM image of the remaining resist profile was taken, which is shown in Fig. 17 where the simulated resist profile obtained by the path-based method is overlaid for comparison. In the simulation, the PSF estimated from the SEM image is employed. In the figure, it is seen that the simulated profile well matches with the actual profile.

7. Summary

A fast path-based method for 3-D resist development simulation of simple patterns has been developed. The proposed method adopts the concept of development paths to simplify the simulation procedure. This allows one to reduce simulation time greatly while achieving sufficiently high accuracy of simulation. In order to optimize the simulation procedure further in terms of simulation time and accuracy, an adaptive procedure has been incorporated into the simulation method, which reduces the simulation time greatly without sacrificing simulation accuracy substantially. Through an extensive simulation, it has been shown that the resist profiles by the proposed method are well matched with those by the cell removal and fast marching methods, while the proposed method takes orders of magnitude less time for simulation, compared to the cell removal and fast marching methods. Also, the accuracy of the proposed method has been verified by an

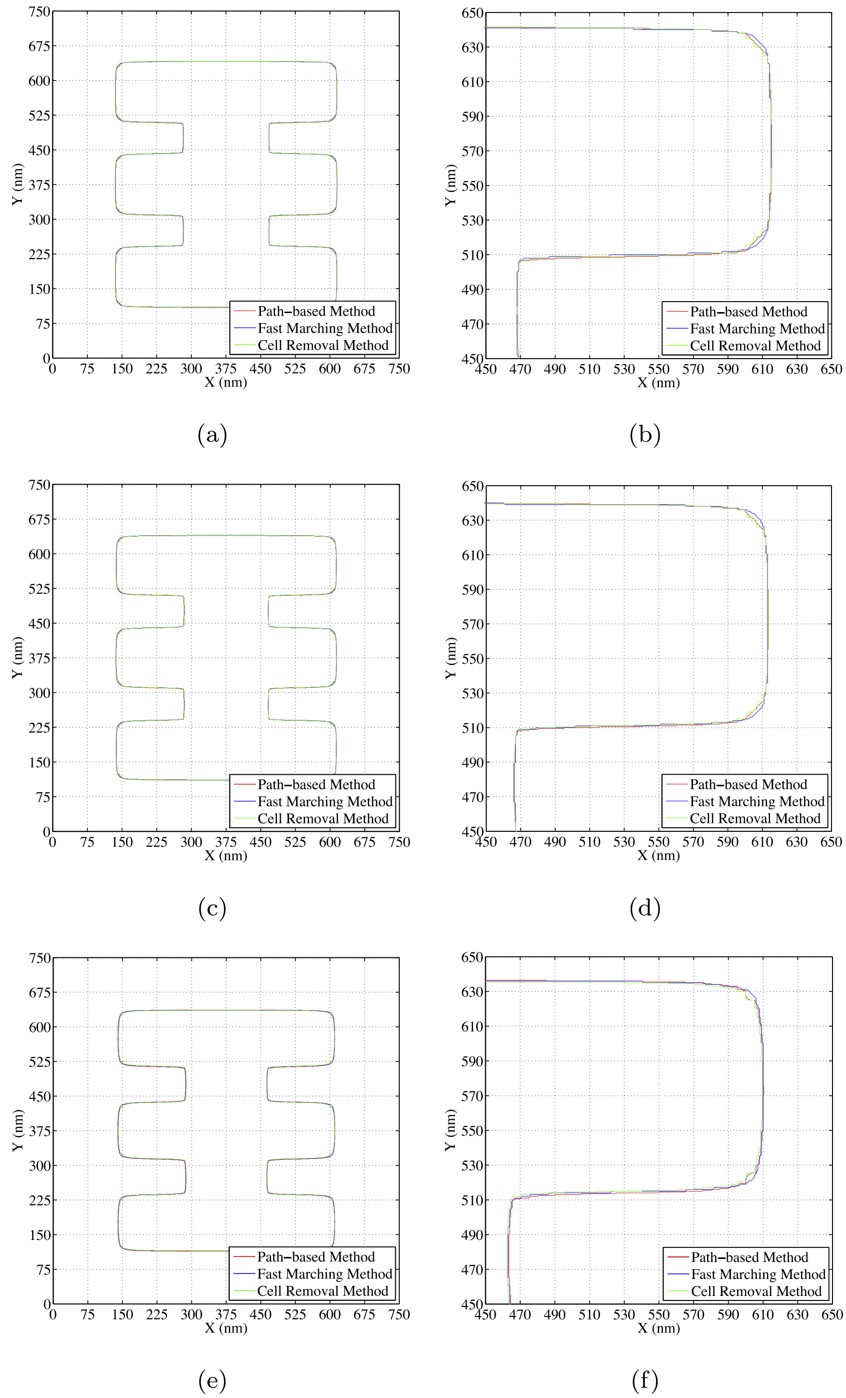

Fig. 15. The remaining resist profiles (top view) for Pattern II at the (a) top, (c) middle, and (e) bottom layers of resist by the path-based, fast marching, and cell removal methods, and the respective zoomed-in details at the (b) top, (d) middle, and (f) bottom layers.

Table 1
Profile difference between the path-based method and each of the cell removal and fast marching methods.

Pattern		Difference of cell removal method			Difference of fast marching method		
ID	Size (nm × nm)	Top (%)	Middle (%)	Bottom (%)	Top (%)	Middle (%)	Bottom (%)
I	500 × 500	0.45	0.53	1.19	0.31	0.73	0.98
II	750 × 750	0.42	0.49	1.54	0.27	0.73	0.73
III	1000 × 1000	0.48	0.78	2.89	0.20	0.65	2.46
IV	150 × 1000	0.70	0.78	3.37	0.30	0.69	0.42
V	250 × 1000	0.70	0.84	2.94	0.19	0.42	1.30
VI	350 × 1000	0.69	1.00	3.28	0.30	1.25	0.56
VII	450 × 1000	0.69	0.95	3.08	0.27	0.86	0.82
VIII	550 × 1000	0.69	1.04	2.41	0.24	1.14	0.86

Table 2
Simulation time of the cell removal and fast marching methods and the path-based method.

Pattern		Cell removal method (s)	Fast marching method (s)	Path-based method (s)		
ID	Size (nm × nm)			One-turn	Two-turn	Adaptive
I	500 × 500	403.86	169.47	6.96	32.52	18.73
II	750 × 750	1869.36	421.82	19.09	64.55	53.58
III	1000 × 1000	5332.55	843.52	27.01	116.07	88.97
IV	150 × 1000	160.72	94.41	4.89	19.50	12.21
V	250 × 1000	594.32	169.07	10.92	39.48	24.94
VI	350 × 1000	1050.71	247.31	13.92	59.99	38.56
VII	450 × 1000	1902.56	332.49	20.03	84.31	52.30
VIII	550 × 1000	2744.31	421.26	22.48	101.25	66.04

Table 3
Speedup of the path-based method over the cell removal and fast marching methods.

Pattern		Speedup over cell removal			Speedup over fast marching		
ID	Size (nm × nm)	One-Turn	Two-Turn	Adaptive	One-Turn	Two-Turn	Adaptive
I	500 × 500	58.03	12.42	21.56	24.35	5.21	9.05
II	750 × 750	97.92	28.96	34.89	22.10	6.53	7.87
III	1000 × 1000	197.43	45.94	59.93	31.23	7.27	9.48
IV	150 × 1000	32.82	8.24	13.16	19.31	4.84	7.73
V	250 × 1000	54.42	15.05	23.83	15.48	4.28	6.68
VI	350 × 1000	75.48	17.51	27.25	17.77	4.12	6.41
VII	450 × 1000	94.99	22.57	36.38	16.60	3.95	6.36
VIII	550 × 1000	122.08	27.11	41.56	18.74	4.16	6.38

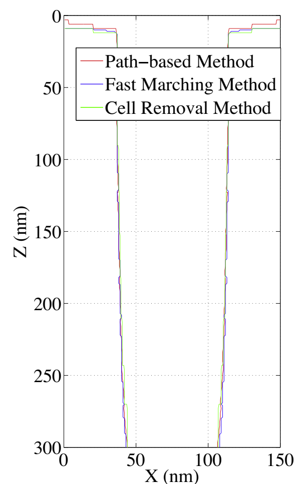

Fig. 16. The remaining resist profiles (cross-section view) for Pattern IV by the path-based, fast marching, and cell removal methods.

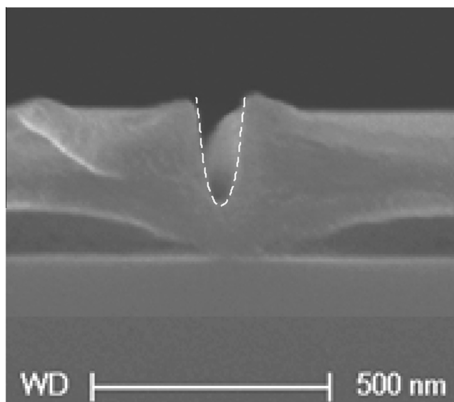

Fig. 17. The cross-section SEM image and the simulated remaining resist profile by the path-based method (white dashed curves) for a long line pattern.

experimental result for a line pattern. The path-based method with one turn is accurate enough for many cases where the size of feature after resist development, e.g., line width, is of main concern. In most cases, at most two turns allowed in each development path would be sufficient. Though the path-based method was developed for simple patterns, it turns out to achieve high accuracy even for more general (complex) patterns. The percentage reduction of simulation time is larger for a larger pattern. Therefore, the proposed path-based method has a good potential to be a practical and efficient alternative to the existing time-consuming methods in applications where fast simulation of resist development is desirable.

Acknowledgement

This work was supported by a research grant from Samsung Electronics Co., Ltd.

References

[1] S.-Y. Lee, K. Anbumony, Microelectron. Eng. 83 (2006) 336.
[2] J. Kim, D.C. Joy, S.Y. Lee, Microelectron. Eng. 12 (2007) 2859.
[3] S.-Y. Lee, K. Anbumony, J. Vac. Sci. Technol. B 25 (2007) 2008.
[4] R. Murali, D.K. Brown, K.P. Martin, J.D. Meindl, J. Vac. Sci. Technol. B 24 (2006) 2936.
[5] T. Okada, J. Fujimori, M. Aida, M. Fujimura, T. Yoshizawa, J. Vac. Sci. Technol. B 29 (2011) 021604.
[6] M. Stepanova, T. Fito, Z. Szab, K. Alti, A.P. Adeyenuwo, J. Vac. Sci. Technol. B 28 (2010) C6C48.
[7] G.P. Patsis, V. Constantoudis, E. Gogolides, Microelectron. Eng. 75 (2004) 297.
[8] T. Schnattinger, E. Br, A. Erdmann, J. Vac. Sci. Technol. B 24 (2006) 3040.
[9] W. Guo, H.H. Sawin, J. Vac. Sci. Technol. A 28 (2010) 250.
[10] L. Lallement, A. Rhallabi, C. Cardinaud, M.C.P. Fernandez, J. Vac. Sci. Technol. A 29 (2011) 051304.
[11] M. Kotera, K. Yagura, H. Niu, J. Vac. Sci. Technol. B 23 (2005) 2775.
[12] J.A. Sethian, Proc. Natl. Acad. Sci. 96 (1996) 1591.
[13] C. Mack, J. Micro/Nanolithogr. MEMS MOEMS 9 (2010) 041202.
[14] M. Osawa, K. Ogino, H. Hoshino, Y. Machida, H. Arimoto, J. Vac. Sci. Technol. B 22 (2004) 2923.
[15] K. Anbumony, S.-Y. Lee, J. Vac. Sci. Technol. B 24 (2006) 3115.
[16] K. Ogino, H. Hoshino, Y. Machida, J. Vac. Sci. Technol. B 26 (2008) 2032.
[17] N. Unal, D. Mahalu, O. Raslin, D. Ritter, C. Sambale, U. Hofmann, Microelectron. Eng. 87 (2010) 940.

[18] Q. Dai, S.-Y. Lee, S.-H. Lee, B.-G. Kim, H.-K. Cho, J. Vac. Sci. Technol. B 29 (2011) 06F314.
[19] Q. Dai, S.-Y. Lee, S.-H. Lee, B.-G. Kim, H.-K. Cho, J. Vac. Sci. Technol. B 30 (2012) 06F307.
[20] C. Mack, J. Vac. Sci. Technol. B 27 (2009) 1123.
[21] Q. Dai, S.-Y. Lee, S.-H. Lee, B.-G. Kim, H.-K. Cho, Microelectron. Eng. 88 (2011) 902.
[22] S. Johnson, Simulation of Electron Scattering in Complex Nanostructures: Lithography, Metrology, and Characterization (Ph.D. Dissertation), Cornell University, Ithaca, NY, 1992.